MINERALOGY OF THE BOCAIUVA IRON METEORITE: A PRELIMINARY STUDY

C. Desnoyers and M. Christophe Michel-Levy
*Laboratoire de Minéralogie-Cristallographie**
Université P. et M. Curie (Paris 6)
4 place Jussieu, 75230 Paris Cedex 05 (France)

I.S. Azevedo, R.B. Scorzelli, and J. Danon
Centro Brasileiro de Pesquisas Físicas
Rio de Janeiro (Brazil)

E. Galvão da Silva
Departamento de Física
Universidade Federal de Minas Gerais
Belo Horizonte (Brazil)

The Bocaiuva iron contains 10 to 15% by volume of silicate inclusions which are surrounded by kamacite (6.5 wt % Ni). The metal shows a Widmanstätten pattern in metal areas devoid of silicates; taenite evolved in plessite fields. The silicate inclusions occur as nodules, and as irregular or chain-like aggregates in which olivine may be rounded or faceted. The magnesian silicates (forsterite, enstatite, diopside) are similar in composition to those of the group IAB irons, whereas the interstitial plagioclase is much more calcic (An 50) than that usually found. Iron sulfide occurs as pyrrhotite and contains 1-2 wt % Cu. Chromite and euhedral magnetite are accessory phases always associated with pyrrhotite. Some patches of pyrrhotite enclose rounded chromite and small plagioclase crystals displaying compositions different from those of the ground mass of the inclusions. Schreibersite shows a compositional variability.

This preliminary study underlines the unusual nature of this iron and raises several questions concerning the genetic relations between silicates, sulfide and metal, and the thermal history of the whole material.

INTRODUCTION

The Bocaiuva iron meteorite, a single piece weighing about 64 kg, was reported in 1962 by a team of geologists of the Instituto de Pesquisas Radioativas at Belo Horizonte, Minas Gerais. The specimen was discovered around 1947 in a farm by Mr. Pedro de Souza Barbosa on the surface of a field, in the locality of Piedade, district of Diamantina.

It was not until 1982 that some interest was brought to it: by Mössbauer spectroscopy, Araujo *et al.* (1983) determined the main constituents while Curvello *et al.* (1983) recognized the unique chemistry of the iron as well as the peculiar composition of the silicates forming the inclusions.

*Associé au C.N.R.S.

ANALYTICAL PROCEDURES

Two slabs were polished with diamond pastes without water to avoid alteration of metal and sulfide. One polished section was etched with a dilute solution of nitric acid in alcohol to bring out structural details in metallic Fe-Ni. The two sections were studied microscopically in reflected light. Mineral analyses were carried out with an automated electron microprobe (CAMEBAX microbeam model, University Paris 6) using crystal spectrometers, following ZAF correction procedures. The beam size was no more than 1 μm (5 μm for feldspar); we used an accelerating voltage of 15 kV, a beam current of 80 nA for the silicates (30 nA for feldspar) and oxides, and 20 kV, 40 nA for the sulfide, phosphide and metal. For each mineral species, the precision of the element contents ($\pm$ Δ in the tables) has been calculated from the total counts of the characteristic X-ray lines and backgrounds. The counting times were 10 to 20 seconds for major elements and 30 seconds for minor elements.

PETROGRAPHY

In the section examined (4 cm^2), the silicate inclusions, 10 to 15% by volume, are made of rounded grains 0.1 to 4 mm, a few are as small as 15 μm; Curvello *et al.* (1983) have seen ''nodules'' up to 1 cm in size. The grains are often associated in chain-like aggregates (Fig. 1), and many of them delineate somewhat parallel trails as if they had been dragged in the molten or at least plastic metal. However, this flow structure is less clear than that described by Buchwald (1975) in the Tucson iron. Some of the largest ''nodules'' observed have been partially broken, with metal filling the cracks.

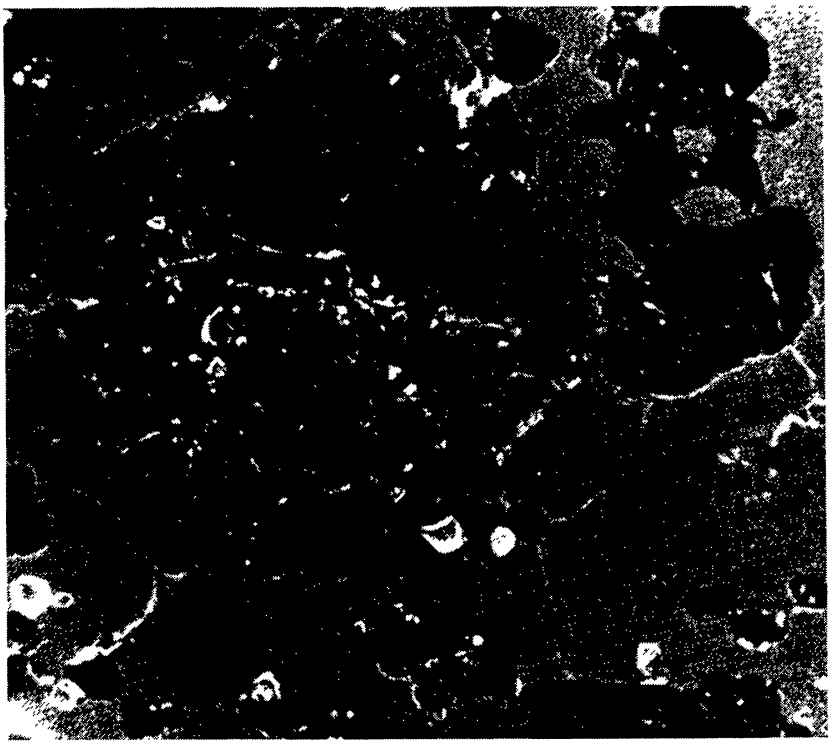

Fig. 1 **S.E.M. view showing a silicate nodule (1 mm wide) sticking to an irregular aggregate besides small chain-like aggregates made of a few crystals. The silicates appear black on this picture and the four following ones.**

Some peripheral olivine of the inclusions and isolated crystals are almost perfectly spherical, but a few ones are well-faceted (Fig. 2). As far as can be seen on the polished sections, the texture of the silicate portion is rather coarse grained. Olivine and pyroxenes tend to develop euhedral crystals. Plagioclase is anhedral and fills the interstices between the femic silicates, as does also the iron sulfide which we designate pyrrhotite based on its chemical and X-ray characteristics. It also occurs as large grains at the metal-silicate boundaries but is never isolated in the metal. Some patches of pyrrhotite, inside the inclusions, enclose chromite and small crystals of plagioclase (Fig. 3). Subhedral chromite grains also occur always associated to pyrrhotite. Some polygonal sections of iron oxide have been observed in pyrrhotite (Fig. 4).

The rock chips are fractured but not heavily shocked. A few empty bubbles may be found, dating from the crystallization of the silicates, together with tiny blebs of metal, sulphide and oxide (Fig. 5).

Owing to the occurrence of the silicate inclusions, the metal did not develop as a single-crystal of γ-iron. The inclusions are swathed by kamacite (Fig. 6). Between the swathing kamacite, the taenite evolved in plessite fields. When the space devoid of silicates is sufficient (a few mm wide), Widmanstätten pattern with 0.1-0.3 mm wide kamacite bands is present (Fig. 7). The plessite areas between these bands may be rather large (up to 1 mm) and of spheroidized, cellular and net types with transitions between the different types in the same area (Figs. 6, 7, 8). The narrow spaces between the

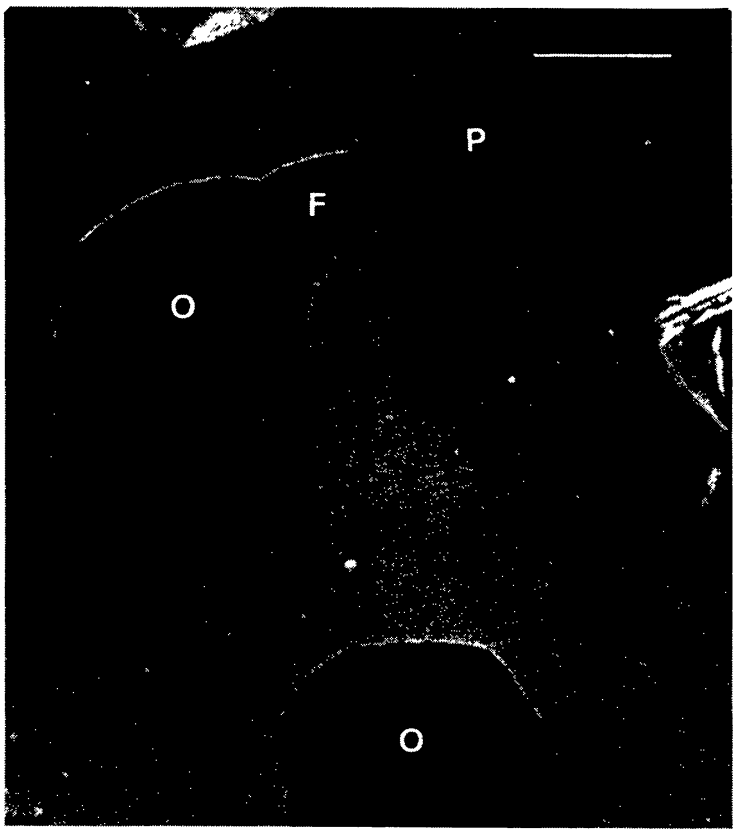

Fig. 2 **Rounded and faceted crystals of silicates. O: olivine, F: feldspar, P: pyroxene (scale bar = 50 μm).**

inclusions are more often martensitic areas and sometimes show a little acicular plessite. Neumann bands are present but not regularly distributed. Schreibersite displays particularly large areas between the silicate inclusions and the swathing kamacite; it also occurs as narrow bands (10 to 50 μm wide) at the kamacite grain boundaries (Fig. 8). No daubreelite nor graphite have been found.

Weathering is probably the origin of the formation of pentlandite rims in some pyrrhotite, and of the iron oxides often found at the metal-silicate boundaries and observed to fill the cracks in metal and silicates.

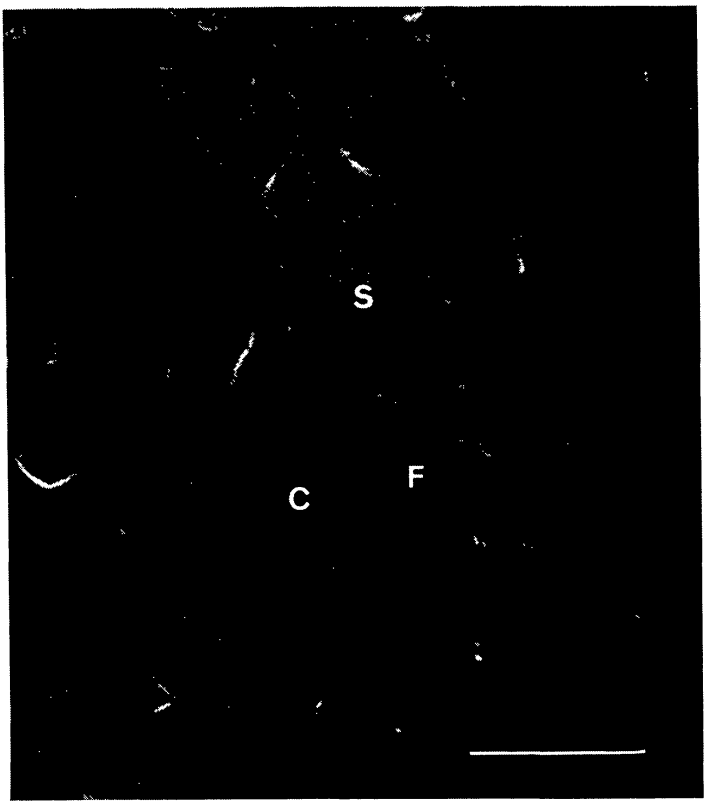

Fig. 3 **Pyrrhotite (S) enclosing rounded chromite (C) and small plagioclase crystal (F) which contain tiny irregular chromite grains (scale bar = 30 μm).**

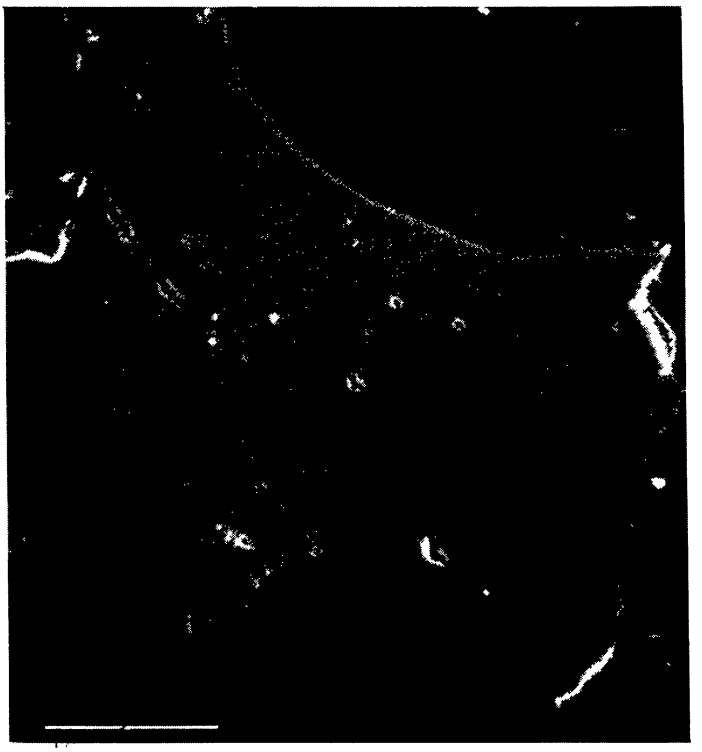

Fig. 4 Euhedral magnetitte (M) embedded in interstitial pyrrhotite (S) between silicates (scale bar = 30 μm).

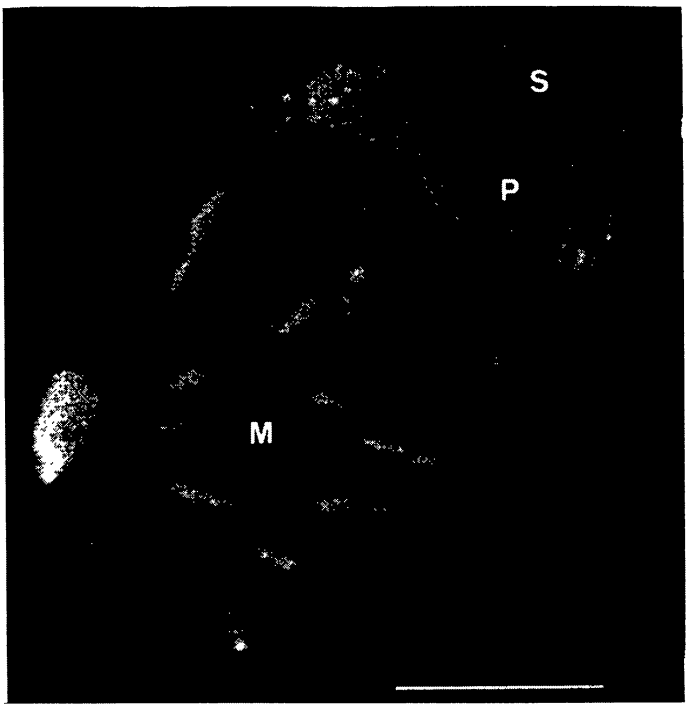

Fig. 5 Small complex inclusion (18 μm wide) in olivine, where iron sulfide (S), kamacite (white), magnetite (M) and schreibersite (P) are coexisting (scale bar = 10 μm).

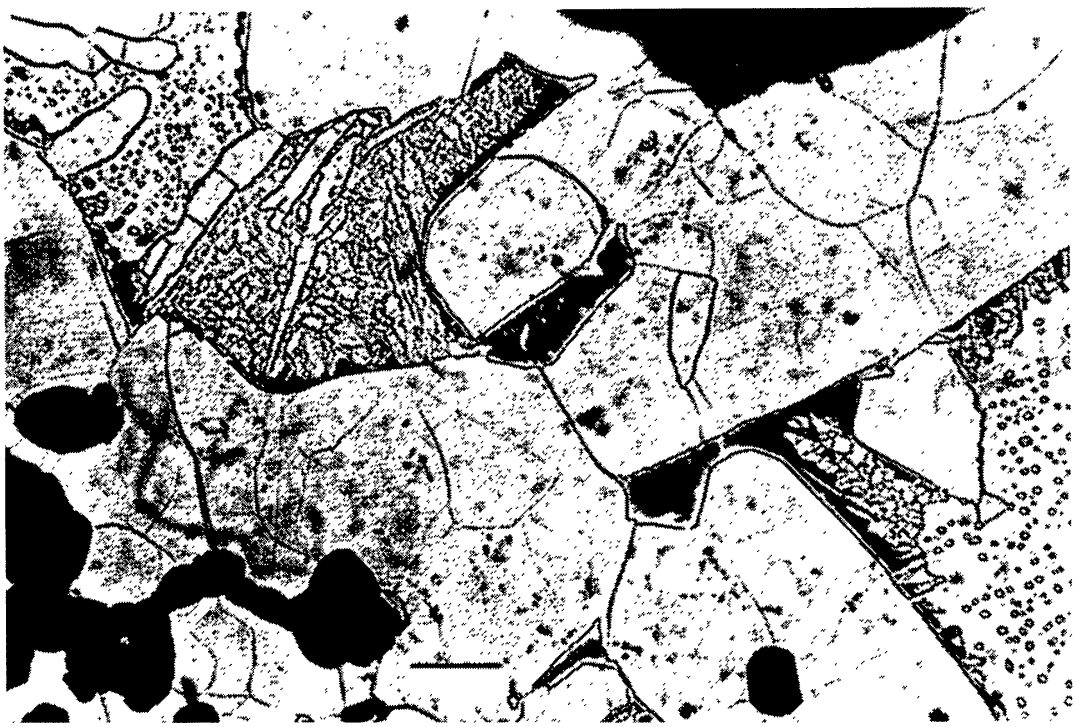

Fig. 6 Kamacite surrounding silicates (a chain-like aggregate at the left low corner, a single olivine crystal right below) between two plessite fields. Reflected light after etching (scale bar = 150 μm).

Fig. 7 Kamcite lamellaes with Widmanstätten pattern, and small fields of cellular plessite. Reflected light after etching (scale bar = 150μm).

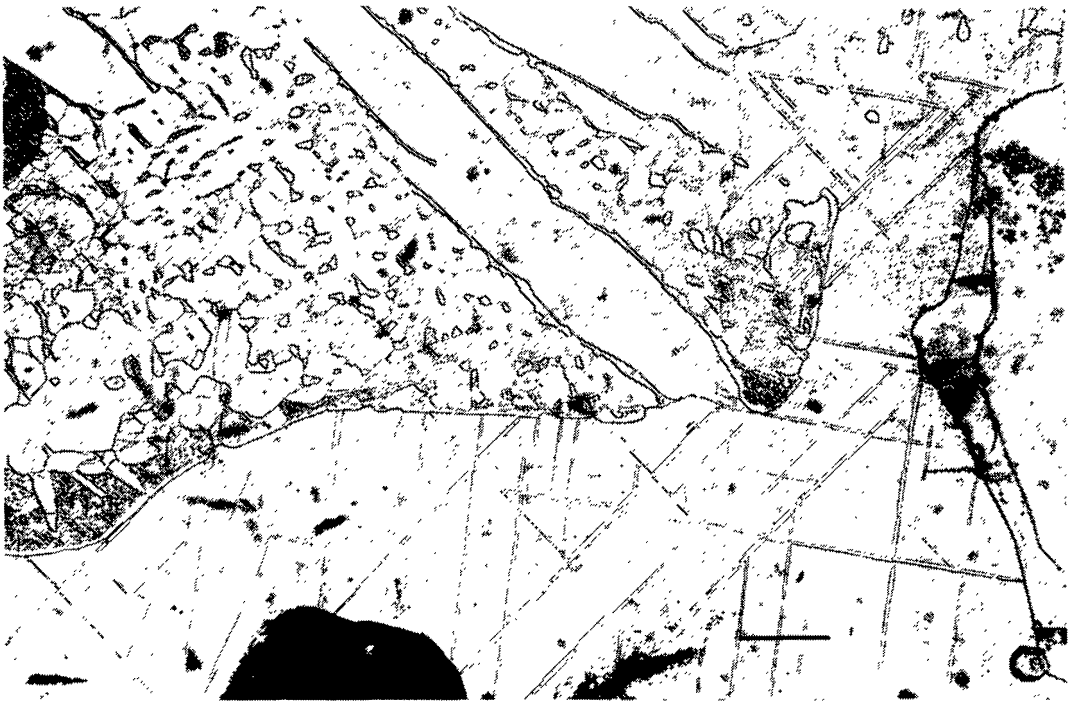

Fig. 8 **Cellular plessite with a border of martensite: kamacite displays Neumann bands; at the right side of the picture lies a schreibersite ribbon. Reflected light after (scale bar = 70 μm).**

MINERAL CHEMISTRY

The representative mineral compositions are grouped in three tables: silicates and chromite (Table 1), pyrrhotite (Table 2), metal and schreibersite (Table 3). When the analyses of several grains of a given species vary within the limits of the accuracy ($\pm$ Δ), solely the average composition is reported with indication of the number of grains analysed.

The silicates of the inclusions are very homogeneous. The fayalite content of olivine ranges from 7.3 to 7.8 mole % from grain to grain and no zoning is discernible. As expected, the calcium content is low (0.03 wt %). The ferrosilite content of orthopyroxene has also a very narrow range (7.1 to 7.8 mole %) with a wollastonite content of 3.1 mole %. Ca-rich pyroxene occurs in rather smaller grains than enstatite; its composition corresponds to diopside (En 53.9, Fs 4.3, Wo 41.8 mole %). The interstitial plagioclase grains (a-table 1) are homogeneous with a constant composition Ab 48.2, Or 1.7, An 50.1 (mole %). The small crystals observed in some pyrrhotite are much more calcic (b-table 1) and show a grain to grain variability: (Ab 38.6-27.7, Or 1.0-0.7, An 60.4-71.6 mole %).

Chromite (b-table 1) associated with small grains of calcic plagioclase (b) in some pyrrhotite is richer in Al_2O_3 and MgO than subhedral chromite grains (a-table 1) associated with pyrrhotite.

Three isotropic polygonal section of iron oxide 20 to 40 μm wide, associated with pyrrhotite have been analyzed. Two of them with 72.0 and 72.2 wt % Fe, correspond to magnetite Fe_3O_4.

Table 1

Microprobe analyses of silicates and chromite in Bocaiuva (wt %)

	Olivine				Enstatite				Diopside			Plag. a		Plag. b		Chr. a		Chr. b
	±Δ	(1)	(10)	(1)	±Δ	(1)	(8)	(1)	±Δ	(2)	±Δ	(7)		(4)		±Δ	(2)	(2)
SiO_2	0.3	41.8	41.7	41.0	0.3	58.1	57.5	57.7	0.3	54.6	0.3	55.8	51.5	50.7				
TiO_2					0.01	0.23	0.24	0.22	0.02	0.61						0.02	0.49	0.98
Al_2O_3					0.03	0.60	0.67	0.66	0.03	1.31	0.2	28.2	31.0	31.6		0.1	1.74	10.2
Cr_2O_3	0.02	0.01	0.03	0.01	0.03	0.65	0.56	0.56	0.04	0.72						0.6	67.0	59.8
FeO	0.12	7.28	7.41	7.77	0.10	4.78	4.98	5.27	0.07	2.75	0.03	0.50	n.d.	n.d.		0.2	20.4	17.0
MnO	0.01	0.25	0.24	0.25	0.01	0.26	0.27	0.28	0.01	0.17						0.03	2.01	1.50
MgO	0.3	51.6	51.6	51.5	0.2	34.1	34.6	34.0	0.2	19.4	0.01	0.07	n.d.	n.d.		0.1	7.92	11.0
CaO	0.01	0.02	0.03	0.03	0.03	1.77	1.70	1.58	0.2	20.9	0.1	10.4	12.6	14.5				
Na_2O									0.02	0.36	0.11	5.53	4.47	3.10				
K_2O											0.02	0.29	0.18	0.11				
Total		100.96	101.01	100.56		100.49	100.52	100.27		100.82		100.79	99.75	100.01			99.56	100.48
	Fa	7.3	7.4	7.8	Fs	7.1	7.3	7.8	Fs	4.3	Ab	48.2	38.6	27.7				
					Wo	3.3	3.1	3.0	Wo	41.8	Or	1.7	1.0	0.7				
					En	89.6	89.6	89.2	En	53.9	An	50.1	60.4	71.6				

Plag. a: interstitial plagioclase between the other silicates; Chr. a: chromite in contact with the silicates and associated to pyrrhotite; Plag. b and Chr. b: small crystals of plagioclase and chromite within some pyrrhotites; n.d.: not determined.

The third with only 67.2 wt % Fe, may depict a transformation stage towards geothite. The iron oxide which often occurs as narrow coating of the metal areas and fills the cracks in metal and silicates averages 90.5 wt % FeO and probably corresponds to maghemite (Fe_2O_3, Fe as FeO: 89.98 wt %). The FeO content of this phase decreases toward the edge of the meteorite to reach 80.4 wt % near the surface, corresponding to geothite (FeO: 80.8 wt %). This feature may indicate the progressive terrestrial weathering.

The iron sulphide contains appreciable amounts of copper and chromium. The atomic percentage calculated from the average composition (51.3 S, 48.7 Fe+Cu+Cr) corresponds to $(Fe+Cu+Cr)_{0.95}S$; according to an X-ray diffractogram of two small hand-picked grains, the d(102) spacing is 2.085 Å, to be compared with the values of 2.093 Å for synthetic FeS (Toulmin and Barton, 1964) and 2.092 Å for troilite isolated from the Tuxtuac chondrite ($Fe_{0.98}S$). Thus, pyrrhotite seems the correct designation for this sulphide.

The interstitial grains (a) in the silicate inclusions and those in contact with the metal (m) display similar Cu content variations, respectively 0.93-2.28 and 1.03-2.03 wt %. The Cu zoning found in two large grains (m) might explain the variation of the Cu content from grain to grain. The pyrrhotites (a) seem to contain more Ni (up to 0.14 wt %) than the pyrrhotites (m) (Ni < 0.04 wt %); however, we must keep in mind the possibility of a contamination by pentlandite although this sulphide was not detected optically in the analysed grains. The patches of pyrrhotite (b) enclosing calcic plagioclase have the same composition as the other grains.

The rare kamacite grains observed in the silicate inclusions (a-table 3) display the same Ni content (~6,5 wt %) as the kamacite (s) surrounding the inclusions, with a slightly higher P content. The two taenite analyses show a 5× higher Cu content than kamacite.

The nickel content of schreibersite ranges from 22.2 to 39.5 wt %. The narrow bands observed in the metal (b-table 3) are Ni-richer than the large areas which occur at the silicate-metal boundaries (a). In the two cases, schreibersite shows constant Zn and Cu contents, respectively 0.73 and 0.14 wt %.

Table 2
Microprobe analyses of pyrrhotite in Bocaiuva (wt %)

	Pyrrhotite (a)				Pyrrhotite (m)							Pyrr. (b)
	±Δ	(3)	(1)	(1)	(2)	(2)	(1)	center	rim	center	rim	(2)
S	0.4	37.3	37.7	37.5	37.6	37.7	37.1	37.1	37.7	37.7	37.7	37.4
Fe	0.5	60.7	60.2	60.0	60.4	60.6	59.6	59.8	59.8	60.8	60.5	59.8
Cu	0.05	0.93	1.11	2.28	1.03	1.23	1.87	1.63	2.03	1.12	1.53	1.48
Cr	0.02	0.50	0.57	0.39	0.37	0.36	0.42	0.41	0.41	0.38	0.37	0.46
Mn	0.01	0.03	0.01	0.01	0.03	0.04	0.01	0.01	0.04	0.01	0.03	0.01
Ni	0.01	0.10	0.13	0.14	0.02	0.01	0.02	0.04	0.03	0.01	0.02	0.16
Zn	0.01	0.03	0.02	—	0.03	—	—	0.02	—	0.02	0.04	—
Total		99.59	99.74	100.32	99.48	99.94	99.02	99.01	100.01	100.04	100.19	99.31

a: interstitial pyrrhotite between the silicates; m: pyrrhotite between the silicates and the surrounding metal; b: pyrrhotite enclosing small crystals of plagioclase and chromite.

Table 3
Microprobe analyses of metal and schreibersite in Bocaiuva (wt %)

	K(a)		K(s)	T	Schreibersite (a)				Schr. (b)	
	±Δ	(2)	(3)	(2)	±Δ	(5)	(3)	(2)	(2)	(2)
S					0.02	0.08	0.06	0.07	0.06	0.06
Fe	0.6	91.9	92.7	81.2	0.4	61.0	56.6	54.3	52.0	43.8
Ni	0.1	6.65	6.51	17.6	0.3	22.2	26.9	29.0	31.5	39.5
Co	0.04	0.35	0.34	0.14	0.02	0.07	0.05	0.04	0.04	0.03
Cu	0.02	0.06	0.05	0.28	0.02	0.14	0.12	0.15	0.13	0.15
Zn	0.01	0.03	0.03	0.03	0.04	0.74	0.74	0.72	0.73	0.72
P	0.01	0.18	0.05	0.02	0.1	15.3	15.5	15.5	15.5	15.4
Total		99.17	99.68	99.27		99.53	99.97	99.78	99.96	99.66

K(a): interstitial kamacite between the silicates; K(s): swathing kamacite surrounding the silicate inclusions; T: taenite. Schreibersite: a — between silicates and metal, b — narrow bands in the metal.

DISCUSSION

Forsterite (Fa 7.4), enstatite (Fs 7.3, En 89.6, Wo 3.1) and diopside (Fs 4.3, En 53.9, Wo 41.8) observed in the silicate inclusions of the Bocaiuva iron constitute a highly equilibrated assemblage. Using the recent model of Lindsley and Andersen (1983), the equilibrium temperature of the pyroxenes seems to be close to 1100°C, within the range of temperatures calculated for inclusions in the IAB irons group from data of Bunch *et al.* (1970). For major elements, olivine and pyroxenes are similar to those reported from silicate inclusions in iron meteorites by Bunch *et al.* (1970). The distribution of Mn between orthopyroxene and clinopyroxene is quite normal: $K_D = X^{Opx}_{MnO} / X^{Ol}_{MnO} = 1.14$ and $K_D = X^{Opx}_{MnO} / X^{Cpx}_{MnO} = 1.6$; Al_2O_3 is rather high but its distribution between the pyroxenes is similar to that in Copiapo type inclusions. However, the chromium distribution is different with $K_D = X^{Opx}_{Cr_2O_3} / X^{Cpx}_{Cr_2O_3} = 0.8$ to be compared to a K_D around 0.2-0.3 usually found in the silicate inclusions in irons after data from Bunch *et al.* (1970) and Bild (1977). On the other hand, this value (0.8) is close to that observed in the silicate inclusions of the hexahedrite Kendall County.

Following the apparent order of crystallization, we must next consider the interstitial plagioclase (a). It differs markedly from that usually observed in the silicate inclusions of irons, being much more calcic (as already noted by Curvello *et al.* (1983) with a composition Ab 48.2, Or 1.7, An 50.1 close to that of plagioclase found by Bunch *et al.* (1970) in one inclusion of Kendall County. The minor elements Fe and Mg have a ratio FeO/MgO = 7 which is remarkable if it is representing the last silicate crystallizing from an initial melt out of which olivine and orthopyroxene crystallized with FeO/MgO approaching 1/7. There are too few data in the literature for comparison; Fe is sometimes measured but nearly never Mg.

An explanation may be that nearly all the magnesium was consumed by crystallization of the magnesian silicates. However, we find still a good deal of magnesium in the chromite (a) which seems to have crystallized later. Another possibility is an increase of fugacity of oxygen, in relation with the increase of activity of sulphur at the end of the crystallization.

Indeed, all the remaining interstices are filled with anhedral pyrrhotite with which chromite (a) is always associated, sometimes magnetite too. In some places, minute graphic intergrowths of sulphide and silicates occur, witness of probably last melted material. In the vicinity of these intergrowths has been found pyrrhotite enclosing chromite (b) and small plagioclases (b) containing tiny chromite inclusions.

Chromite (a) has a normal composition compared to those reported by Bunch *et al.* (1970) from silicate inclusions in IAB irons group, but chromite (b) is outside the group and much more aluminous than chromite (a). The same tendency is found for the small plagioclases (b) An 60.4-An 71.6 compared to An 50.1 for the ground mass andesine. The genetic relation between these two different plagioclases is not clear. One puzzling thing is that the solidus of plagioclase An 60 to 70 is some 50°C higher than the solidus of plagioclase An 50. We have little information concerning the sulphide-silicate melts. However, according to experiments of Tilley *et al.* (1964) with mixtures of FeS + basaltic rock powders, the melting temperature of the feldspar seems to be clearly lowered by the addition of FeS. Moreover, when quenched, the sulphide melt accompanying the silicate melt crystallized in a mixture of pyrrhotite and magnetite according to Kullerud and Yoder (1968) who noticed that the composition of the sulphide is buffered by the silicates.

That is perhaps the reason of the occurrence of pyrrhotite instead of troilite in Bocaiuva, and why the magnetite observed is probably primary and not a weathering product. Indeed, it is very rare that pyrrhotite is the principal sulphide phase in meteorites. The fact that pyrrhotite crystallized in Bocaiuva instead of troilite may explain that copper (1-2 wt %) has been accepted in the sulphide as a solid solution. The large solubility of copper in pyrrhotite has been underlined by von Gehlen and Kullerud (1962), up to 2 wt % at 600°C) and by Yund and Kullerud (1966, up to 4 wt % at 700°C). The range of Cu content of the Bocaiuva pyrrhotite implies that this sulphide crystallized from 600°C towards lower temperatures and did not reach equilibrium.

This lack of equilibrium is also observed in the metal phases of Bocaiuva since no detectable trace of tetrataenite has been found in the Mössbauer spectrum, Araujo *et al.* (1983). This spectrum is similar to that of Cratheus 1950 for which large metallographic cooling rates ($\sim$ 300°C $\times$ 10ηy) have been estimated, J.F. Albertsen (Thesis, University of Copenhagen, 1980).

CONCLUSION

This preliminary study of the Bocaiuva iron raises more questions than it solves.

1 — Are there genetic relations between the silicate inclusions and the metal?

The tiny opaque drops found entirely embedded in the silicates seem to display the same particularities as the main opaque phases. These blebs may be primary, dating from the initial crystallization of the silicates. They may be secondary: immiscible drops trapped by the silicates subsequent to a possible melting stage of silicates in the molten metal, or blebs having penetrated in the silicates through cracks subsequently healed by recrystallization.

2 — How and at what temperature were the silicates included in the metal?

The silicates might have consisted of sand-size particles at the time they were included coming from a disaggregated and probably homogeneous material (remember that the 64 kg iron has only been sampled at one end until now, so the homogeneity cannot be ascertained). If the metal was molten, it had to cool in short time to prevent gravitational separation and large melting of silicates. If it was not molten, it had to be plastic enough to enable short silicate chains to aggregate. 1400 to 1200°C may be reasonable temperatures to produce both rounding and faceting of the silicate (i.e. olivine). At these temperatures, iron sulfide was liquid, penetrating the rock chips and remelting some silicates. Whether it belonged initially to the silicate portions or was provided by the metal is not clear. In favor of the latter option might be the small amount of sulfur remaining in the schreibersite which exsolved from the metal, and the occurrence of copper both in the iron sulfide and schreibersite and, at a very low level, in the metal.

3 — How can it be explained that the silicate equilibrium has been frozen around 1100°C in a cooling metal which exhibits a Widmanstätten pattern?

This question concerns all the irons with silicate inclusions since they all show equilibrium temperatures between 900 and 1200° according to Bunch *et al.* (1970). The silicate assemblage of Bocaiuva inclusions, equilibrated around 1100°C, should require a subsequent rapid cooling till the temperature where the diffusion in the silicates is stopped. The occurrence of kamacite bands in the ferro-nickel should imply then a slow cooling when the whole material reaches 600°C. However, the absence of tetrataenite and the features of the Mössbauer spectrum would require again a rapid cooling under 300°C (i.e. extraction from the parent body by impact). The period of slow cooling between 600 and 300°C could be shortened considering the last model computed by Narayan and Goldstein (1983).

Clearly, much more detailed investigations are necessary to provide a comprehensive answer to these questions.

ACKNOWLEDGMENTS

We thank Dr. Clecio Murta for her collaboration in obtaining the meteorite sample. We also thank the reviewers for their constructive remarks.

REFERENCES

Araujo, S.I., J. Danon, R.B. Scorzelli, I.S. Azevedo, and E. Galvão da Silva, 1983. Mössbauer study of silicates and metal phases of the Bocaiuva meteorite. *Meteoritics* **18**, 261.

Bild, R.W., 1977. Silicate inclusions in group IAB irons and a relation to the anomalous stones Winona and Mt. Morris (Wis.). *Geochim. Cosmochim. Acta* **41**, 1439-1456.

Buchwald, V.F., 1975. Handbook of iron meteorites. University of California Press.

Buchwald, V.F., 1977. The mineralogy of iron meteorites. *Phil. Trans. Roy. Soc. London* **286**, 453-491.

Bunch, T.E., K. Keil, and E. Olsen, 1970. Mineralogy and petrology of silicate inclusions in iron meteorites. *Contrib. Mineral. Petrol.* **25**, 297-340.

Curvello, W.S., D.J. Malvin, and J.T. Wasson, 1983. Bocaiuva, a unique silicate inclusion bearing iron meteorite. *Meteoritics* **18**, 285.

Kellerud, G. and H.S. Yoder, 1968. Sulfide-silicate relations. *Carnegie Inst. Yearbook* **63**, 92-97.

Lindsley, D.H. and D.J. Andersen, 1983. A two pyroxene thermometer. *Jour. Geophys. Res.* **88A**, 887-906.

Malvin, D.J., W. Daode, and J.T. Wasson, 1984. Chemical classification of iron meteorites — X; Multielement studies of 43 irons, resolution of group III E from III AB, and evaluation of Cu as taxonomic parameter. *Geochim. Cosmochim. Acta* **48**, 785-804.

Narayan, C. and J.I. Goldstein, 1983. A major revision of the iron meteorite cooling rates. *Abstract Meteoritical Society*.

Tilley, C.E., H.S. Yoder, and J.F. Schairer, 1964. New relations on melting of basalts. *Carnegie Inst. Yearbook* **63**, 92-97.

Toulmin, P. and P.B. Barton, 1964. A thermodynamic study of pyrite and pyrrhotite. *Geochim. Cosmochim. Acta* **28**, 641-671.

Von Gehlen, K. and G. Kullerud, 1962. Pyrrhotite-pyrite-chalcopyrite relations. *Carnegie Inst. Wash. Yearbook* **61**, 154-155.

Manuscript received 4/9/84